A Dynamic Model for Smart Water Distribution Networks

Stefan Kaltenbacher[1], David B. Steffelbauer[2], Marco Cattani[3], Martin Horn[1], Daniela Fuchs-Hanusch[2] and Kay Römer[3]
[1]Institute of Automation and Control, Inffeldgasse 21B/I
[2]Institute of Urban Water Management, Stremayrgasse 10/I
[3]Institute of Technical Informatics, Inffeldgasse 16/I
Graz University of Technology, Austria
[1]*s.kaltenbacher,* [2]*david.steffelbauer,* [3]*m.cattani,* [1]*martin.horn,* [2]*fuchs-hanusch,* [3]*roemer@tugraz.at*

ABSTRACT

While background leakages accounting for substantial water losses in supply networks remain undetectable, human reaction to even visible pipe bursts is insufficiently slow. We lose precious time in which not only water losses but severe damage to the surrounding infrastructure could be prevented. These leakages can often be identified only during the minimum night flow and so repair work is delayed by days, causing intermittent water supply and outages. Increasing costs and the importance to ensure supply security require further measures.
Therefore, the application of holistic algorithms controlling proportional valves and pumps allows to act instantaneously on failures by isolating affected pipe sections and by reducing the pressure in that region. With the target to apply classical control theory and yet avoid too complex formulations, this paper presents a dynamic model using no more parameters than a typical, steady-state EPANET model. By means of a sophisticated network description, we modify the rigid water column theory in terms of pressure-driven demands. Other than traditional methods, this approach enables nodal consumptions to dynamically change inner system states such as pressure or flow values. Within this method, the nodal elevation undergoes proper treatment in the model equations and further ensures that pressure values will not become negative as one may have experienced in EPANET.

Keywords: Hydraulic Network Modeling, Flow Dynamics, Water Distribution Control Systems

1 INTRODUCTION

Before using software to perform computer simulations on hydraulic networks, research on network modeling also focused on transients in the 1970s and 1980s [1, 2]. With the launch of EPANET (1993) though, CPU-intensive first dynamic models were slow and thus outperformed by a tool which applied steady-state descriptions only, but calculated flow and pressure values fast and free of charge. However, the application of enhanced numeric algorithms for solving differential equations led to vast speed and stability improvements, whereas the cost for computing power decreased rapidly. We have now already surpassed a tipping point, where sufficient computing power to solve dynamic models for more complex hydraulic networks is available.
Furthermore, new technologies evolving, e.g., from the research on *Internet of Things*, provide fast and reliable wireless data communication over large distances [3]. These new protocols facilitate the deployment of pressure and flow sensors by reducing cost and labor, avoiding cost-intensive digging for cable installations. New opportunities to couple sensor and actuator devices with hydraulic

simulation models will make it possible not only to monitor, but also to actively control networks in real time. This framework sets new hardware and software challenges which can finally be overcome in a cost-effective manner.

2 A DYNAMIC, YET RIGID APPROACH

Pressure transients aside, the *rigid water column* theory has distinct advantages over the *elastic* theory [1, 2] for describing hydraulic transients in pipes, if applied to whole networks. By restricting the space resolution to entire pipes and avoiding additional parameters such as the pipe elasticity or fluid compressibility, computational effort and complexity are reduced substantially. In the context of this *rigid* theory, the ordinary differential equation (ODE)

$$\frac{dQ}{dt}\frac{l}{gA} = (h+z)\big|_{s=0} - (h+z)\big|_{s=l} - \overbrace{f_{\mathrm{DW}}(Q)\frac{l\,|Q|\,Q}{2dgA^2}}^{h_{\mathrm{DW}}(Q)} - \overbrace{k_m|Q|\,Q}^{h_m(Q)} \tag{1}$$

describes the fluid flow Q through a pipe with cross section area A, diameter d and length l. Symbols z and h indicate the elevation and the pressure head at starting point $s = 0$ and the end point $s = l$ of this pipe respectively, thereby defining the flow direction. The constant g characterizes the gravitational acceleration. The *Darcy-Weisbach* term h_{DW}, describing friction at the inner wall of the pipe's surface, includes factor f_{DW} [4] which itself depends on the Reynolds number (hence on Q) and therefore has to be distinguished between the three flow regimes. Minor losses h_m including friction coefficient k_m and losses $h_{\mathrm{loss}} = h_{\mathrm{DW}} + h_m$ in general are proportional to the quadratic flow, whereas using the absolute value helps to retain the right sign in case the flow changes its direction.

Network Formulation. Collecting n_l pipe flows in $\boldsymbol{x}_Q \in \mathbb{R}^{n_l}$, n_l head losses in $\boldsymbol{h}_{\mathrm{loss}} \in \mathbb{R}^{n_l}$, n_j nodal pressure heads in $\boldsymbol{h} \in \mathbb{R}^{n_j}_{\geq 0}$, n_j elevations in $\boldsymbol{z} \in \mathbb{R}^{n_j}_{\geq 0}$, n_j nodal consumptions in $\bar{\boldsymbol{q}} \in \mathbb{R}^{n_j}_{\geq 0}$ and n_s sources in $\boldsymbol{h}_s \in \mathbb{R}^{n_s}_{\geq 0}$ (given by explicit pressure head values) will then help to establish a compact network formulation. The nodal equations in the network can be written in the linear form [4]

$$\boldsymbol{A}\boldsymbol{x}_Q = \bar{\boldsymbol{q}} \tag{2}$$

utilizing the so-called *incidence* matrix $\boldsymbol{A} \in \mathbb{Z}^{n_j \times n_l}_{\{-1,0,1\}}$ which consists of minus ones, zeros and ones only. After defining $\boldsymbol{c}_l := g[A_1/l_1 \quad \dots \quad A_{n_l}/l_{n_l}]^T \in \mathbb{R}^{n_l}_{>0}$ a vector containing information about pipe parameters, the network's ODEs gain the following compact shape

$$\frac{d\boldsymbol{x}_Q}{dt} = -\mathrm{diag}\,(\boldsymbol{c}_l)\,\boldsymbol{A}^T(\boldsymbol{h}+\boldsymbol{z}) - \mathrm{diag}\,(\boldsymbol{c}_l)\,\boldsymbol{h}_{\mathrm{loss}}(\boldsymbol{x}_Q) + \boldsymbol{C}_s\boldsymbol{h}_s. \tag{3}$$

Source matrix $\boldsymbol{C}_s = \mathrm{diag}\,(\boldsymbol{c}_l)\,\tilde{\boldsymbol{C}}_s$ includes $\tilde{\boldsymbol{C}}_s \in \mathbb{Z}^{n_l \times n_s}_{\{-1,0,1\}}$ which has non-zero entries in rows where sources connect to flows $x_{Q,i}$. When deriving the nodal equations (2) with respect to time, the ODEs (3) can be inserted, which then allows to calculate the nodal pressure heads

$$\boldsymbol{h}+\boldsymbol{z} = \left(\boldsymbol{A}\mathrm{diag}\,(\boldsymbol{c}_l)\,\boldsymbol{A}^T\right)^{-1}\left[\boldsymbol{A}\mathrm{diag}\,(\boldsymbol{c}_l)\left(\tilde{\boldsymbol{C}}_s\boldsymbol{h}_s - \boldsymbol{h}_{\mathrm{loss}}(\boldsymbol{x}_Q)\right) - \frac{d\bar{\boldsymbol{q}}}{dt}\right]. \tag{4}$$

Thanks to its diagonal structure, matrix $\boldsymbol{L} := \boldsymbol{A}\text{diag}\,(\boldsymbol{c}_l)\,\boldsymbol{A}^T$ remains positive definite for all possible network configurations.

Network Equations. To avoid approximating the time derivatives of nodal consumptions $\bar{\boldsymbol{q}}$ in equation (4), as their behavior is only known rudimentarily, we move $\bar{\boldsymbol{q}}$ into the derivative of $\boldsymbol{x}_Q$. Starting with inserting expression (4) into the ODEs (3) and then moving $\frac{d\bar{\boldsymbol{q}}}{dt}$ to the left hand side yields

$$\frac{d}{dt}\left(\boldsymbol{x}_Q - \text{diag}\,(\boldsymbol{c}_l)\,\boldsymbol{A}^T\boldsymbol{L}^{-1}\bar{\boldsymbol{q}}\right) = \left(\boldsymbol{I} - \text{diag}\,(\boldsymbol{c}_l)\,\boldsymbol{A}^T\boldsymbol{L}^{-1}\boldsymbol{A}\right)\left(\boldsymbol{C}_s\boldsymbol{h}_s - \text{diag}\,(\boldsymbol{c}_l)\,\boldsymbol{h}_{\text{loss}}(\boldsymbol{x}_Q)\right) \tag{5}$$

which is feasible as $\text{diag}\,(\boldsymbol{c}_l)\,\boldsymbol{A}^T\boldsymbol{L}^{-1}$ is constant. $\boldsymbol{I}$ characterizes the identity matrix. For solving the ODEs (5), the right-hand side is fed to an ODE solver and the result increased by the term $\text{diag}\,(\boldsymbol{c}_l)\,\boldsymbol{A}^T\boldsymbol{L}^{-1}\bar{\boldsymbol{q}}$, involving nodal consumptions.

Formulation Characteristics. The case when the number of junctions equals the number of pipes $n_j = n_l$ draws attention to matrix

$$\boldsymbol{I} - \text{diag}\,(\boldsymbol{c}_l)\,\boldsymbol{A}^T\left(\boldsymbol{A}\text{diag}\,(\boldsymbol{c}_l)\,\boldsymbol{A}^T\right)^{-1}\boldsymbol{A} \overset{n_j=n_l}{=} \boldsymbol{0} \tag{6}$$

which becomes zero and thus results in the complete loss of the dynamic, meaning that the linear nodal equations (2) are sufficient for solving the network. In order to let the ODEs (5) be solvable, the initial conditions $\boldsymbol{x}_Q(t_0)$ need to be consistent $\boldsymbol{A}\boldsymbol{x}_Q(t_0) \overset{!}{=} \bar{\boldsymbol{q}}(t_0)$, which is a non-trivial request as this equation system usually has multiple solutions. One weak spot of this formulation can be seen in the set-up of pressure heads (4), as the influence of the nodal elevation $\boldsymbol{z}$ cancels out completely. However, this is no unique property, also in steady-state models (*EPANET2*), the nodal elevation has no direct effect on the network equations (conservation of mass and energy [5, 4]). This problem is usually being bypassed by subtracting $\boldsymbol{z}$ after the pressure head vector $\boldsymbol{h}$ has been calculated. As one may know from working with *EPANET2*, receiving a warning indicating negative pressure values is a rather common experience, although this statement is incorrect from a physical perspective.

2.1 Pressure-Driven Demand (PDD)

By explicitly specifying the course of $\bar{\boldsymbol{q}}(t)$ the appropriate consumer flow is always subtracted from the respective node, even in case there is not enough pressure to satisfy the demand. These problems are well known and communities already focused on modifications such that only target or reference values are considered. Various works [6, 7, 8] propose extensions by introducing quantities such as the desired pressure (satisfying the target consumption) or available pressure at the respective node. Within many methods the consumption behavior has no direct influence on inner system states. Formulations using iterative methods [9] or optimization problems [10] were needed to adjust inner pressure and flow values to the varying consumption.

In reality, the consumer outflow depends on the local pressure level and on the consumer's pipe characteristics. When equating potential- to kinetic energy and then multiplying with cross section

area A, the discharge relation

$$q = r(\alpha)A\sqrt{2gh} \tag{7}$$

extended by an additional coefficient $r(\alpha)$ is obtained. This coefficient is capable of adjusting the consumption q much like one regulates the water flow by opening or closing a water tap. In this context α represents the degree of tap opening. Although several empirical relations for calculating r depending on the flow condition and on the *Reynolds* number have been identified [11], we pursue another approach. After adding the orifice equation (7) to the network formulation, we focus on the control of consumption[1] $\boldsymbol{q}$ to follow a specified target consumption by manipulating $\boldsymbol{r}$. By using a control algorithm to adjust $r \in]0, 1]$, it is not advisable to use complex empiric relations for finding suitable orifice coefficients, since the tap opening α is unknown anyway.

PDD Network Formulation. By applying the *Hadamard Operator* $\circ$ [12] to represent element-wise multiplications ($\boldsymbol{H}, \boldsymbol{J} \in \mathbb{C}^{m\times n}$) $[\boldsymbol{H} \circ \boldsymbol{J}]_{ij} = H_{ij}J_{ij}$ or exponentiations $[\boldsymbol{H}^{\circ^{-1}}]_{ij} = H_{ij}^{-1}$ for $1 \le i \le m, 1 \le j \le n$ in a more compact manner, the orifice equation (7) transforms to

$$\boldsymbol{q} = \sqrt{2g}\left(\boldsymbol{r} \circ \boldsymbol{a}_q \circ \boldsymbol{h}_q^{\circ^{1/2}}\right) = \sqrt{2g}\,\mathrm{diag}\left(\boldsymbol{a}_q \circ \boldsymbol{h}_q^{\circ^{1/2}}\right)\boldsymbol{r}. \tag{8}$$

Utilizing subset $\mathbb{R}_{[a,b]} = \{k \in \mathbb{R} \mid k \in [a, b]\}$, $\boldsymbol{r} \in \mathbb{R}_{[\epsilon_r,1]}^{n_q}$ characterizes the outflow coefficients of n_q consumers and $\boldsymbol{a}_q \in \mathbb{R}_{>0}^{n_q}$ a vector of cross section areas belonging to n_q consumer openings. $\boldsymbol{h}_q \in \mathbb{R}_{\ge 0}^{n_q}$ represents $n_q \le n_j$ elements of pressure head $\boldsymbol{h}$ specifying locations of nodal consumptions greater zero only $\boldsymbol{q} \in \mathbb{R}_{>0}^{n_q}$. When inverting equation (8) in terms of $\boldsymbol{h}_q$, the coefficients $\boldsymbol{r}$ appear in the denominator, meaning that the pressure at consumers could potentially become infinite if this coefficient tends to zero. To circumvent this case, the range of $\boldsymbol{r}$ was bounded $[\epsilon_r, 1]$ appropriately. Hence, for simulating (almost) zero consumptions within $\boldsymbol{q}$ at the n_q specified consumer points, we can only let the coefficients $\boldsymbol{r} \to \epsilon_r$ approach zero. Due to the numeric robustness of applied solvers, the intentional error will be so small that the results are not affected significantly. This is the reason why we separate nodal equations (2) into

$$\begin{array}{c} n_q \text{ consumer nodes} \\ \boldsymbol{R}_q\bar{\boldsymbol{q}} = \boldsymbol{q} \qquad \boldsymbol{R}_q \in \mathbb{Z}_{\{0,1\}}^{n_q\times n_j} \end{array} \quad \text{and} \quad \begin{array}{c} n_j - n_q \text{ non-consumer nodes} \\ \bar{\boldsymbol{R}}_q\bar{\boldsymbol{q}} = \boldsymbol{0} \qquad \bar{\boldsymbol{R}}_q \in \mathbb{Z}_{\{0,1\}}^{(n_j-n_q)\times n_j}. \end{array} \tag{9}$$

The same separation is conducted in the nodal pressure heads, i.e.

$$\boldsymbol{R}_q\boldsymbol{h} = \boldsymbol{h}_q \qquad \text{and} \qquad \bar{\boldsymbol{R}}_q\boldsymbol{h} = \bar{\boldsymbol{h}} \qquad \bar{\boldsymbol{h}} \in \mathbb{R}^{n_j-n_q}. \tag{10}$$

The transpose of *Hadamard Matrices* $\boldsymbol{R}_q$ and $\bar{\boldsymbol{R}}_q$ is closely related to their (pseudo-) inverse. Consequentially, their dominant property

$$\boldsymbol{h} = \boldsymbol{R}_q^T\boldsymbol{h}_q + \bar{\boldsymbol{R}}_q^T\bar{\boldsymbol{h}} \tag{11}$$

helps to separate the dynamic equation system (3). The resulting n_j independent nodal equations

[1] note the change in notation $\boldsymbol{q} \neq \bar{\boldsymbol{q}}$

$$\boldsymbol{R}_q \boldsymbol{A} \boldsymbol{x}_Q = \sqrt{2g} \left(\boldsymbol{r} \circ \boldsymbol{a}_q \circ \boldsymbol{h}_q^{\circ 1/2} \right), \tag{12a}$$

$$\bar{\boldsymbol{R}}_q \boldsymbol{A} \boldsymbol{x}_Q = \boldsymbol{0} \tag{12b}$$

are sufficient to determine all unknown pressure heads. By inverting equation (12a), n_q elements of $\boldsymbol{h}$ can already be obtained. Since $\boldsymbol{q} = \boldsymbol{R}_q \boldsymbol{A} \boldsymbol{x}_Q$ has to be greater zero, it is recommended to intercept the sign of consumptions $\boldsymbol{q}$ by means of $\left|\boldsymbol{R}_q \boldsymbol{A} \boldsymbol{x}_Q\right| \circ (\boldsymbol{R}_q \boldsymbol{A} \boldsymbol{x}_Q) \stackrel{!}{=} (\boldsymbol{R}_q \boldsymbol{A} \boldsymbol{x}_Q)^{\circ 2}$ and abort the simulation if $\boldsymbol{q}$ becomes negative (cf. eq. (12a)). The necessity to simulate consumptions $\boldsymbol{q} > 0$ allows the pressure heads to remain $\boldsymbol{h} \geq 0$ as long as we select a proper value for the boundary, e.g. $\epsilon_r = 10^{-7}$. To be fair, this only proves true if sources $\boldsymbol{h}_s$ are strong enough for at least satisfying (almost) zero consumptions within $\boldsymbol{q}$, in which case the discharge coefficients become $\boldsymbol{r} = [1 \quad \dots \quad 1]^T \epsilon_r$.
We obtain the remaining $n_j - n_q$ heads (13) after deriving equation (12b), inserting ODEs (3) and identity (11), and then moving terms successively to the right hand side.

$$\bar{\boldsymbol{h}} = \left(\bar{\boldsymbol{R}}_q \boldsymbol{L} \bar{\boldsymbol{R}}_q^T \right)^{-1} \bar{\boldsymbol{R}}_q \boldsymbol{A} \left(\boldsymbol{C}_s \boldsymbol{h}_s - \boldsymbol{c}_l \circ \boldsymbol{h}_{\text{loss}}(\boldsymbol{x}_Q) - \text{diag}\,(\boldsymbol{c}_l)\, \boldsymbol{A}^T (\boldsymbol{R}_q^T \boldsymbol{h}_q + \boldsymbol{z}) \right) \tag{13}$$

Matrix $\bar{\boldsymbol{R}}_q \boldsymbol{L} \bar{\boldsymbol{R}}_q^T$ is regular, since we know that $\bar{\boldsymbol{R}}_q$ has full rank $n_j - n_q$, following its introduction purpose in definition (9) and (10). After summarizing the results of equation (3), (12a) and (13), the differential equation system

$$\boxed{\begin{aligned} \frac{d\boldsymbol{x}_Q}{dt} &= -\text{diag}\,(\boldsymbol{c}_l)\, \boldsymbol{A}^T (\boldsymbol{R}_q^T \boldsymbol{h}_q + \bar{\boldsymbol{R}}_q^T \bar{\boldsymbol{h}} + \boldsymbol{z}) - \boldsymbol{c}_l \circ \boldsymbol{h}_{\text{loss}}(\boldsymbol{x}_Q) + \boldsymbol{C}_s \boldsymbol{h}_s \\ \boldsymbol{h}_q &= \frac{1}{2g} \left(\boldsymbol{a}_q^{\circ -2} \circ \left|\boldsymbol{R}_q \boldsymbol{A} \boldsymbol{x}_Q\right| \circ (\boldsymbol{R}_q \boldsymbol{A} \boldsymbol{x}_Q) \circ \boldsymbol{r}^{\circ -2} \right) \\ \bar{\boldsymbol{h}} &= \left(\bar{\boldsymbol{R}}_q \boldsymbol{L} \bar{\boldsymbol{R}}_q^T \right)^{-1} \bar{\boldsymbol{R}}_q \boldsymbol{A} \left(\boldsymbol{C}_s \boldsymbol{h}_s - \boldsymbol{c}_l \circ \boldsymbol{h}_{\text{loss}}(\boldsymbol{x}_Q) - \text{diag}\,(\boldsymbol{c}_l)\, \boldsymbol{A}^T (\boldsymbol{R}_q^T \boldsymbol{h}_q + \boldsymbol{z}) \right) \end{aligned}} \tag{14}$$

with consumption $\boldsymbol{q} = \boldsymbol{R}_q \boldsymbol{A} \boldsymbol{x}_Q$ actually resembles *differential algebraic equations* (DAEs). However, by utilizing matrix $\boldsymbol{B} := \text{diag}\,(\boldsymbol{c}_l)\, \boldsymbol{A}^T \bar{\boldsymbol{R}}_q^T \left(\bar{\boldsymbol{R}}_q \boldsymbol{L} \bar{\boldsymbol{R}}_q^T \right)^{-1} \bar{\boldsymbol{R}}_q \boldsymbol{A}$ the more compact form

$$\frac{d\boldsymbol{x}_Q}{dt} = (\boldsymbol{I} - \boldsymbol{B}) \left[\boldsymbol{C}_s \boldsymbol{h}_s - \boldsymbol{c}_l \circ \boldsymbol{h}_{\text{loss}}(\boldsymbol{x}_Q) - \text{diag}\,(\boldsymbol{c}_l)\, \boldsymbol{A}^T \left(\frac{1}{2g} \boldsymbol{R}_q^T \left(\boldsymbol{a}_q^{\circ -2} \circ (\boldsymbol{R}_q \boldsymbol{A} \boldsymbol{x}_Q)^{\circ 2} \circ \boldsymbol{r}^{\circ -2} \right) + \boldsymbol{z} \right) \right] \tag{15}$$

emphasizes its ordinary character. In contrast to eq. (6) (pressure independent demands), the dynamics

$$\boldsymbol{I} - \text{diag}\,(\boldsymbol{c}_l)\, \boldsymbol{A}^T \bar{\boldsymbol{R}}_q^T \left(\bar{\boldsymbol{R}}_q \boldsymbol{A} \text{diag}\,(\boldsymbol{c}_l)\, \boldsymbol{A}^T \bar{\boldsymbol{R}}_q^T \right)^{-1} \bar{\boldsymbol{R}}_q \boldsymbol{A} \stackrel{n_j = n_l}{\neq} \boldsymbol{0} \tag{16}$$

of this formulation generally remain intact in case the number of pipes equals the number of nodes. This holds true with the exception of the case $n_q = n_j$, when all nodes are consumers, resulting in $\boldsymbol{I} - \boldsymbol{B} \stackrel{n_j = n_l = n_q}{=} \boldsymbol{0}$. Again, nodal equations (2) are sufficient for solving the network in this special case. Provided that the distribution network completely lacks loops, steady-state models retain some legitimacy although the dynamic character further revealed by the pressure-dependent demands and the consumer separation.

3 CASE STUDY AND RESULTS

For illustrative purposes, we consider a hydraulic network consisting of two loops (Figure 1), $n_l = 5$ pipe flows, $n_j = 3$ nodes and one ($n_s = 1$) reservoir R supplying a constant pressure head of $h_s = 30$ m. Nodal elevations are $\boldsymbol{z} = [z_{\text{N1}} \quad z_{\text{N2}} \quad z_{\text{N3}}]^T = [0 \quad 5 \quad 10]^T$ m. The two consumers at node N2 and N3 are consuming $q_{\text{N2}} = 1$, resp. $q_{\text{N3}} = 0.7$ l/s. Nodal equations, consumer and non-consumer equations are defined as follows.

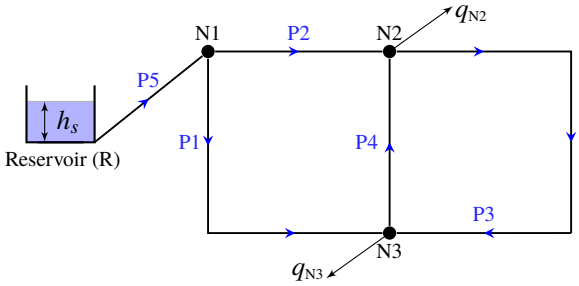

Figure 1. *Two-Loop Network.*

$$\overbrace{\begin{bmatrix} -1 & -1 & 0 & 0 & 1 \\ 0 & 1 & -1 & 1 & 0 \\ 1 & 0 & 1 & -1 & 0 \end{bmatrix}}^{\boldsymbol{A}} \overbrace{\begin{bmatrix} Q_{\text{P1}} \\ \vdots \\ Q_{\text{P5}} \end{bmatrix}}^{\boldsymbol{x}_Q} = \overbrace{\begin{bmatrix} 0 \\ q_{\text{N2}} \\ q_{\text{N3}} \end{bmatrix}}^{\bar{\boldsymbol{q}}}, \qquad \overbrace{\begin{bmatrix} 0 & 1 & 0 \\ 0 & 0 & 1 \end{bmatrix}}^{\boldsymbol{R}_q} \bar{\boldsymbol{q}} = \overbrace{\begin{bmatrix} q_{\text{N2}} \\ q_{\text{N3}} \end{bmatrix}}^{\boldsymbol{q}}, \qquad \overbrace{\begin{bmatrix} 1 & 0 & 0 \end{bmatrix}}^{\bar{\boldsymbol{R}}_q} \bar{\boldsymbol{q}} = 0$$

Considering parameter vector $\boldsymbol{c}_l = 9.81 \cdot \overbrace{0.04^2\pi/4}^{A_{\text{P1}}=\ldots=A_{\text{P5}}} \cdot (\overbrace{[20 \quad 10 \quad 30 \quad 10 \quad 10]^T}^{l_{\text{P1}} \quad l_{\text{P2}} \quad l_{\text{P3}} \quad l_{\text{P4}} \quad l_{\text{P5}}})^{\circ -1}$, source matrix $\boldsymbol{C}_s$ becomes $\boldsymbol{C}_s = \text{diag}\,(\boldsymbol{c}_l)\,[0 \quad 0 \quad 0 \quad 0 \quad 1]^T = \text{diag}\,(\boldsymbol{c}_l)\,\tilde{\boldsymbol{C}}_s$. We select $\boldsymbol{a}_q$ by equating maximal consumer openings to cross section areas of original pipes $\boldsymbol{a}_q = [A_{\text{P2}} \quad A_{\text{P3}}]^T$. Minor loss coefficients are set to zero $\boldsymbol{k}_m = \boldsymbol{0}$, whereas roughness coefficients are $\boldsymbol{\epsilon}_{\text{DW}} = [0.0015 \quad 3 \quad 0.0015 \quad 3 \quad 0.0015]^T$ mm (factors $\boldsymbol{f}_{\text{DW}}$ were varied according to [5]). We simulate a step response by increasing $\boldsymbol{r}$ from $\epsilon_r = 10^{-7}$ to $\boldsymbol{r} = [0.041 \quad 0.026]^T$ instantaneously at $t = 1$s.

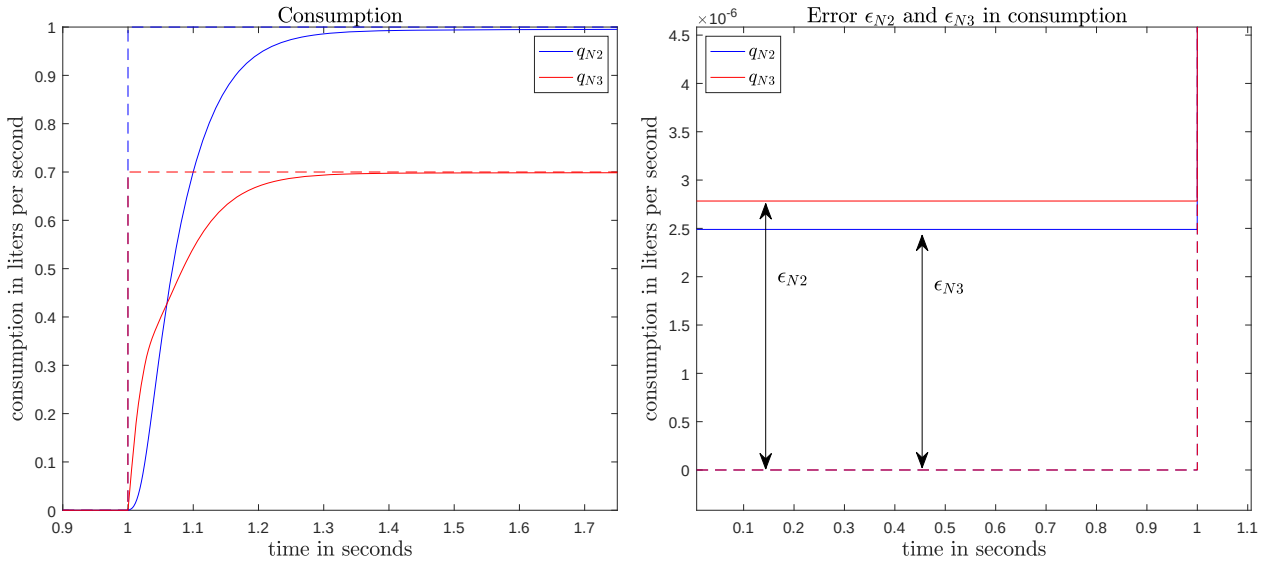

Figure 2. *Simulated consumption in EPANET2 (dashed line) and MATLAB (solid line).*

Regarding Figure 2, the sudden increase in consumer outflow coefficients $\boldsymbol{r}$ causes the water mass inside the network to react inertially such that consumptions gradually reach desired values. The

mutual influence of q_{N2} and q_{N3} during their dynamic transition can be seen at $t \approx [1, 1.03]$s, where q_{N3} increases rapidly until q_{N2} reaches maximal slope and forces q_{N3} to slow down. Hereby consumption q_{N3} presumably starts off first as pipe P2 and P4 have significantly higher roughness coefficients. Furthermore, as distance $R \xrightarrow{P5} N1 \xrightarrow{P1} N3 \xrightarrow{P3} N2$ is twice the distance $R \xrightarrow{P5} N1 \xrightarrow{P1} N3$, h_{N3} recovers slower than h_{N3} ($t \approx [1, 1.03]$s) from the sudden pressure decrease when opening consumers (see Figure 3). On the right hand side of Figure 2 it can be seen that the lower boundaries $\epsilon_{N2} = \epsilon_r A_{P2}\sqrt{2gh_{N2}(t < 1s)} \approx 2.5 \cdot 10^{-6}$ l/s and $\epsilon_{N3} = \epsilon_r A_{P3}\sqrt{2gh_{N3}(t < 1s)} \approx 2.8 \cdot 10^{-6}$ l/s in consumption $\boldsymbol{q}$ are sufficiently small and thus insignificant for the simulation results.

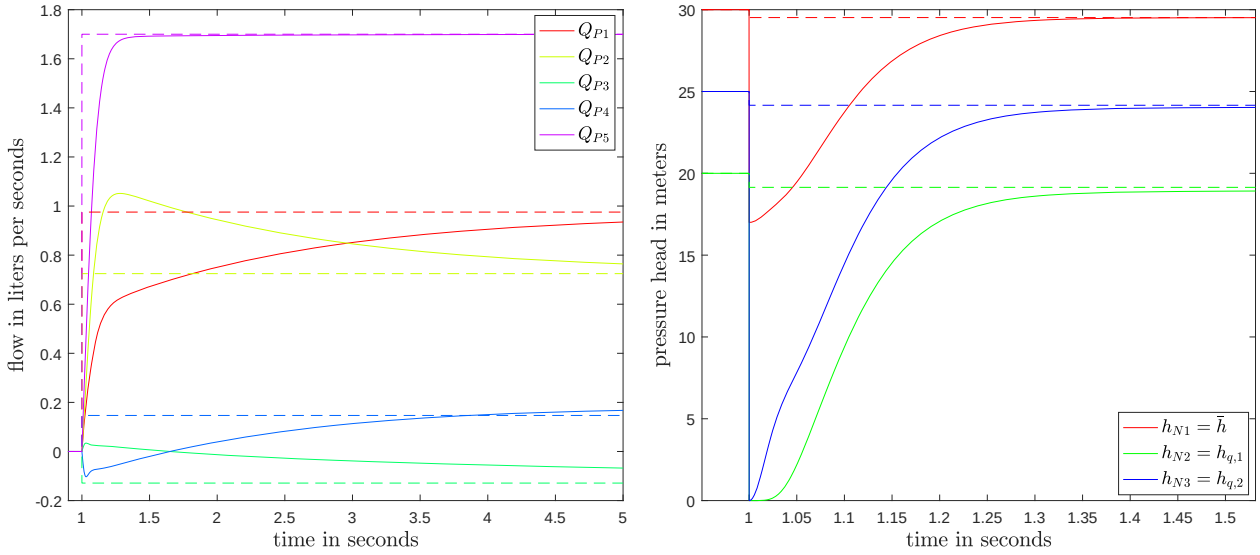

Figure 3. *Simulated flow and pressure head in EPANET2 (dashed line) and MATLAB (solid line).*

As shown in Figure 3, the results of the dynamic model (14) converge to the steady-state values computed by EPANET2. Consequentially, it is reasonable to assume, with the absence of any prove, that loop equations (conservation of energy [4]) used in steady-state models are satisfied implicitly. The jump in pressure heads can be directly attributed to derived model equations (14), where the jump in coefficients $\boldsymbol{r}$ directly penetrates $\boldsymbol{h}_q$.

The orifice coefficients $\boldsymbol{r} = [0.041 \quad 0.026]^T$ were determined by a static control algorithm which will be subject to following publications, however, the simulation related to Figure 2 and 3 was conducted without feedback loop.

Running MATLAB code on a low power notebook (release 2015), the computation for solving 120s in simulation took 1s in real time with standard settings. We applied stiff solver ODE15s which is capable of adjusting the step size efficiently in case of rapid changes in a large number of state variables $\boldsymbol{x}_Q$.

4 CONCLUSION AND OUTLOOK

In this paper we derived a dynamic description of water networks and performed simulations on a small example, illustrating that results of EPANET and MATLAB are identical in steady-state. We currently take high-resolution measurements in an experimental water distribution network (see [13]) while exciting transients in the hydraulic system. A detailed comparison between measurements and

simulation results will further help to validate the model and study its behavior.
The new system class allows the application of methods from control theory, which are fairly new in this field, to manipulate flow transients. Algorithms on the principle of exact linearization, model predictive control, etc. could coordinate the actuation of proportional valves and pumps, and thus bear the potential to drastically reduce the total water loss as well as the overall energy consumption.

References

[1] Fox J. A. *Hydraulic Analysis of Unsteady Flow in Pipe Networks*. THE MACMILLAN PRESS LTD, 1977.

[2] Watters Z. Gary. *Modern Analysis and Control of Unsteady Flow in Pipelines*. ANN ARBOR SCIENCE, 1979.

[3] Cattani M., Boano C. A., Steffelbauer D. B., Kaltenbacher S., Günther M., Römer K., Fuchs-Hanusch D. and Horn M. "*Adige: An Efficient Smart Water Network based on Long-Range Wireless Technology*". In: 3rd International Workshop on Cyber-Physical Systems for Smart Water Networks (SysWater), Pittsburgh, US (2017).

[4] Walski T., Chase D., Savic D., Grayman W., Beckwith S. and Koelle E. *Advanced Water Distribution Modeling and Management*. Haested Press, 2003 – 2004.

[5] Rossman A. Lewis. *EPANET 2 User Manual*. United States Environmental Protection Agency (EPA), 2000.

[6] Fujiwara O. and Li J. "*Reliability analysis of water distribution networks in consideration of equity, redistribution and pressure dependent demand*". In: *Water Resource Research* 34 (1998), pp. 1843–1850.

[7] Muranho J., Ferreira A., Sousa J., Gomes A., and Sá Marques A. "*Pressure-Dependent Demand and Leakage Modelling With an EPANET Extension - WaterNetGen*". In: *Procedia Engineering* 89 (2014), pp. 632–639.

[8] Jung B. S., Boulos P. F. and Wood D. J. "Effect of pressure-sensitive demand on surge analysis". In: *Journal American Water Works Association* (2009), pp. 100–111.

[9] Giustolisi 0., Savic D., and Kapelan Z. "*Pressure-Driven Demand and Leakage Simulation for Water Distribution Networks*". In: Journal of Hydraulic Engineering (2008), pp. 626–635.

[10] Piller O., Bremond B., Poulton M. "*Least Action Principles Appropriate to Pressure Driven Models of Pipe Networks*". In: World Water Congress (2004).

[11] Jelali M. and Kroll A. *Hydraulic Servo-systems: Modelling, Identification and Control*. Springer-Verlag London Ltd., 2003.

[12] Million E. "The Hadamard Product". In: Creative Commons (2007).

[13] Günther M., Steffelbauer D. B. and Fuchs-Hanusch D. "*Fault detection data creation using an experimental water distribution system*". In: 3rd Conference on Control and Fault-Tolerant Systems (SysTol), Barcelona, Spain (2016).